K-SPACE TRAJECTORY DESIGN FOR REDUCED MRI SCAN TIME

Shubham Sharma, K.V.S. Hari

Electrical Communication Engineering Dept.
Indian Institute of Science
Bengaluru, India

Geert Leus

Circuits and Systems
Dept. of Microelectronics, EEMCS
Delft University of Technology
Delft, Netherlands

ABSTRACT

The development of compressed sensing (CS) techniques for magnetic resonance imaging (MRI) is enabling a speedup of MRI scanning. To increase the incoherence in the sampling, a random selection of points on the k-space is deployed and a continuous trajectory is obtained by solving a traveling salesman problem (TSP) through these points. A feasible trajectory satisfying the gradient constraints is then obtained by parameterizing it using state-of-the-art methods. In this paper, a constrained convex optimization based method to obtain feasible trajectories is proposed. The method is motivated by the fact that the readout time is proportional to the number of sample points and includes the lengths of the segments of the trajectory in the cost function to obtain variable length trajectories. The proposed method provides a reduction in readout time by more than 50% for random-like trajectories with an improvement of about 1.5 dB in peak signal-to-noise ratio (PSNR) and 0.0762 in structural similarity (SSIM) index on average for a realistic brain phantom MRI image adopting single-shot trajectories.

Index Terms— MRI, k-space trajectories, compressed sensing

1. INTRODUCTION

Magnetic resonance imaging (MRI) is a noninvasive diagnostic imaging technique [1]. It consists of a large homogeneous magnet (B_0) and three linear gradient coils along with RF transceiver coils. The gradients are used for spatial encoding and the signal maps directly to the 2D/3D frequency domain, commonly known as the k-space in the MRI community. The image matrix $\mathbf{X}$ is reconstructed by simply taking the 2D inverse Fourier transform ($\mathcal{F}^{-1}$) of the 2D k-space data $\mathbf{Y}$, i.e., $\mathbf{X} = \mathcal{F}^{-1}(\mathbf{Y})$. The traversed k-space from a given gradient function $\mathbf{g}(t) = (g_x(t), g_y(t), g_z(t))$ is obtained as $\mathbf{k}(t) = \gamma \int_0^t \mathbf{g}(\tau)d\tau$ [1] where γ is the gyromagnetic ratio (42.58MHz/T for Hydrogen). The gradients are limited in magnitude ($G_{\max}$) and slew rate ($S_{\max}$) due to physical and safety constraints. Hence, while designing a k-space trajectory, the gradient constraints need to be satisfied.

The time during which the k-space data is measured is called the readout time. Reducing the MRI acquisition time has been a subject of research in the MRI community and methods like compressed sensing (CS) [2] and parallel imaging [3, 4, 5] have been proposed. CS techniques facilitate the recovery of highly undersampled signals if the signal is sparse by itself or in a transform domain and the measurements are observed incoherently. There has been a lot of research on efficient sparsifying transform designs such as those based on curvelets [6] and trained dictionary-based methods [7]. In this paper, we consider the less studied problem of a feasible trajectory design under the CS framework with the aim to reduce readout time without compromising the reconstruction performance. Traditionally, undersampling is achieved by optimally choosing phase encodings for Cartesian sampling [2]. Similarly, for non-Cartesian trajectories such as spiral and radial, undersampling is achieved by using a reduced number of interleaves [2, 8] and spokes [9], respectively. However, these trajectories do not really conform with the traditional CS theory and new methods are being developed to improve the performance of MRI systems [10, 11]. To overcome the coherence barrier in the MRI problem due to high global coherence between the wavelet and Fourier bases, variable density (VD) sampling is used which is motivated by the fact that the coherence decreases with an increasing frequency or wavelet scale [10]. Hence, the center of the k-space (low-frequency region) is more densely sampled as compared to the boundaries (high-frequency region).

The density $\propto 1/|k|^2$ is experimentally observed to perform better than the theoretically optimal density for Fourier and wavelet bases [11]. However, to suit the physical constraints of the gradients, a smooth and continuous trajectory is needed. A recently proposed method to find a trajectory through the randomly sampled points, although uncommon in practice, is by solving a traveling salesman problem (TSP) [12]. Such TSP-based trajectories are considered in this work as they provide the shortest path through the sampled points and hence, ensure a small readout time. The readout time, during which the k-space data is sampled, depends on the (potentially varying) speed at which the curve is traversed as well as the fixed sampling period T_s. If there is finally a total of n sample points, the readout time is $T = nT_s$. Note in this context that the final sample points are different from the original sample points obtained from the VD sampling. If the TSP curve is traversed with a con-

ICASSP 2020

stant speed, it may be infeasible to be implemented in an MRI machine because of its sharp turns. There are various methods in the literature that provide ways to traverse a given infeasible trajectory [13, 14, 15]. The time-optimal control (TOC) method [13] uses optimal control theory to provide the fastest way to traverse the trajectory satisfying the gradient constraints. For trajectories like the TSP trajectory with sharp corners more time and hence more samples are needed at the corners and this, in turn, increases the total readout time. A projection-based method [15], in which the given trajectory is first parameterized and then projected on the set of feasible trajectories is used as a basis to build the proposed method. The motivation for using the projection method is that it allows the trajectory to deviate from the original trajectory, hence smoothing out the sharp turns in a TSP trajectory. In this paper, we propose an alternative method than [15] by including the lengths of the segments of the trajectory in the optimization problem. This gives the designer the flexibility to alter the readout time by choosing a different weighting parameter. This paper assumes that the effects of field inhomogeneity, T2* decay and other irregularities including gradient errors due to eddy currents are negligible and can be ignored.

2. TRAJECTORY DESIGN

Assume the set of feasible trajectories with k_x- and k_y-coordinates ($\mathbf{s}_x \in \mathbb{R}^m$ and $\mathbf{s}_y \in \mathbb{R}^m$, respectively) stacked in a vector $\mathbf{s} \in \mathbb{R}^{2m} = [\mathbf{s}_x^T \ \mathbf{s}_y^T]^T$ is given by

$$\mathcal{S}^m = \{\mathbf{s} \in \mathbb{R}^{2m} : \|\mathbf{D}_1^{(2)}\mathbf{s}\|_\infty \leq T_s\alpha, \|\mathbf{D}_2^{(2)}\mathbf{s}\|_\infty \leq T_s^2\beta\} \quad (1)$$

where $\alpha = \gamma G_{\max}$, $\beta = \gamma S_{\max}$, $\mathbf{D}_1^{(2)}$ is the block diagonal matrix constructed from the first order difference matrix $\mathbf{D}_1$ and $\mathbf{D}_2^{(2)}$ is the block diagonal matrix constructed from the second order difference matrix $\mathbf{D}_2$, $\mathbf{D}_2 = -\mathbf{D}_1^T\mathbf{D}_1$. The feasible trajectory from the projection method [15] is then given by

$$\mathbf{s}_{\mathrm{P}} = \arg\min_{\mathbf{s} \in \mathcal{S}^m} \quad \frac{1}{2}\|\mathbf{s} - \mathbf{c}_{\mathrm{par}}\|_2^2 \quad (2)$$

where $\mathbf{c}_{\mathrm{par}} \in \mathbb{R}^{2m}$ is the trajectory obtained after constant velocity parameterization (CVP) of the original trajectory $\mathbf{c} \in \mathbb{R}^{2n}$, $n < m$. CVP is equivalent to arc-length parameterization for a constant sampling frequency. CVP essentially interpolates $\mathbf{c}$ by introducing new sample points such that the consecutive points attain a velocity v proportional to a fraction of the maximum velocity $v_{\max} = \gamma G_{\max}$. This increases the total number of sample points compared to the original points that were used to make the TSP trajectory, which increases the readout time. However, to ensure a satisfactory reconstruction of an image one does need more sample points than in the original TSP trajectory. Keeping this in mind, we propose to find a feasible trajectory, hereby called the constrained length trajectory (COLT) by first solving the following constrained convex optimization problem
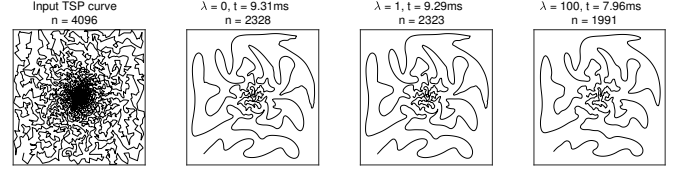

Fig. 1: Trajectories for different values of the weighting parameter λ in the COLT method for a TSP curve found using 4096 randomly sampled points. The readout time and the number of sample points are denoted by t and n, respectively. $v = 0.15v_{\max}$.

$$\mathbf{s}_{\mathrm{COLT}} = \arg\min_{\mathbf{s} \in \mathcal{S}^n} \quad \frac{1}{2}\|\mathbf{s} - \mathbf{c}\|_2^2 + \frac{\lambda}{2}\|\mathbf{D}_1^{(2)}\mathbf{s}\|_2^2 \quad (3)$$

where $\lambda \in \mathbb{R}^+$ is a weighting parameter and $\|\mathbf{D}_1^{(2)}\mathbf{s}\|_2^2$ is the sum of squares of the Euclidean distances between consecutive points of $\mathbf{s}$. This imposes a cost on the segments of the trajectory $\mathbf{s}$ which in turn decides the overall length of the trajectory. Hence, we project the given trajectory $\mathbf{c}$ without any parameterization (i.e., it contains the original points of the TSP trajectory) onto the set of feasible trajectories and include a cost on the length of the segments of the trajectory. The resultant trajectory $\mathbf{s}_{\mathrm{COLT}}$ will have the same number of sample points as that of $\mathbf{c}$. As the final step, to increase the number of sample points and to reduce the velocity variation in consecutive points, $\mathbf{s}_{\mathrm{COLT}}$ is parameterized using a constant velocity v which is a factor of $v_{\max}$, denoted $\mathbf{s}'_{\mathrm{COLT}}$. A variable number of sample points, and hence a variable readout time is achieved by this parameterization. This is because the higher the value of the weighting parameter, the smaller the number of samples points after constant velocity parameterization, and thus the shorter the readout time. So, in effect, the second term in the cost function provides control over the readout time which provides the motivation to include this additional term in the cost function. The gradient constraints in this case will still be satisfied as the velocity chosen for parameterization is feasible and the trajectory is smooth without sharp edges. Fig. 1 shows the effect of varying λ for a 4098 point TSP trajectory with initial points taken from the density $\propto 1/|k|^2$. With increasing λ, the trajectories tend to become smoother. Note that (3) can be easily extended to 3D.

Convex optimization techniques in the dual space are used to optimally solve the problem in (3). Notations are borrowed from [15] for consistency. Using the standard definitions of the dual norm and the indicator function, for the set $B_\alpha = \{\mathbf{x} \in \mathbb{R}^n, \|\mathbf{x}\|_\infty \leq \alpha\}$, the indicator function is obtained as

$$I_{B_\alpha}(\mathbf{x}) = \sup_{\mathbf{y} \in \mathbb{R}^n} \mathbf{x}^T\mathbf{y} - \alpha\|\mathbf{y}\|_1 \quad (4)$$

Hence, the optimization problem (3) can be formulated in the dual domain as

Algorithm 1: COLT Algorithm

Input: $\mathbf{c} \in \mathbb{R}^{2n}$, $\lambda > 0$, $\epsilon > 0$, L, α, β
Initialization: $\mathbf{q}^{(0)} = (\mathbf{q}_1^{(0)^T} \ \mathbf{q}_2^{(0)^T})^T = (\mathbf{0}^T \ \mathbf{0}^T)^T$,
  $\mathbf{y}^{(0)} = \mathbf{q}^{(0)}$, $t = 1/L$, $\mathbf{e} = \mathbf{c}$, $k = 0$
while $\|\mathbf{e}\|_2^2 \leq \epsilon$ **do**
  $\quad k = k + 1$
  $\quad \mathbf{q}^{(k)} = \mathrm{prox}_{F,t}(\mathbf{y}^{(k-1)} + t\nabla F(\mathbf{y}^{(k-1)}))$
  $\quad \mathbf{y}^{(k)} = \mathbf{q}^{(k)} + \frac{k-1}{k+2}(\mathbf{q}^{(k)} - \mathbf{q}^{(k-1)})$
  $\quad \mathbf{e} = \mathbf{q}^{(k)} - \mathbf{q}^{(k-1)}$
end
Output: $\mathbf{s}_{\mathrm{COLT}} = \mathbf{s}^*(\mathbf{q}_1^{(k)}, \mathbf{q}_2^{(k)})$

$$\min_{\mathbf{s}} \frac{1}{2}\|\mathbf{s} - \mathbf{c}\|_2^2 + \frac{\lambda}{2}\|\mathbf{D}_1^{(2)}\mathbf{s}\|_2^2 + \sup_{\mathbf{q}_1,\mathbf{q}_2}\big[(\mathbf{D}_1^{(2)}\mathbf{s})^T\mathbf{q}_1 \\ + (\mathbf{D}_2^{(2)}\mathbf{s})^T\mathbf{q}_2 - \alpha\|\mathbf{q}_1\|_1 - \beta\|\mathbf{q}_2\|_1\big] \quad (5)$$

$$= \sup_{\mathbf{q}_1,\mathbf{q}_2} \min_{\mathbf{s}} \frac{1}{2}\|\mathbf{s} - \mathbf{c}\|_2^2 + \frac{\lambda}{2}\|\mathbf{D}_1^{(2)}\mathbf{s}\|_2^2 + ((\mathbf{D}_1^{(2)}\mathbf{s})^T\mathbf{q}_1 \\ + (\mathbf{D}_2^{(2)}\mathbf{s})^T\mathbf{q}_2 - \alpha\|\mathbf{q}_1\|_1 - \beta\|\mathbf{q}_2\|_1 \quad (6)$$

The minimization expression above can be written as

$$F(\mathbf{q}_1, \mathbf{q}_2) = \min_{\mathbf{s}} \frac{1}{2}\|\mathbf{s} - \mathbf{c}\|_2^2 + \frac{\lambda}{2}\|\mathbf{D}_1^{(2)}\mathbf{s}\|_2^2 \\ + (\mathbf{D}_1^{(2)}\mathbf{s})^T\mathbf{q}_1 + (\mathbf{D}_2^{(2)}\mathbf{s})^T\mathbf{q}_2 \quad (7)$$

whose solution $\mathbf{s}^*(\mathbf{q}_1, \mathbf{q}_2)$ can be computed as

$$\mathbf{s}^*(\mathbf{q}_1, \mathbf{q}_2) = (I + \lambda\mathbf{D}_1^{(2)^T}\mathbf{D}_1^{(2)})^{-1}(\mathbf{c} - \mathbf{D}_1^{(2)^T}\mathbf{q}_1 - \mathbf{D}_2^{(2)^T}\mathbf{q}_2) \quad (8)$$

The optimization problem in (6) can then be reduced to

$$\inf_{\mathbf{q}_1,\mathbf{q}_2}\big(-F(\mathbf{q}_1, \mathbf{q}_2) + G(\mathbf{q}_1, \mathbf{q}_2)\big) \quad (9)$$

where $G(\mathbf{q}_1, \mathbf{q}_2) = \alpha\|\mathbf{q}_1\|_1 + \beta\|\mathbf{q}_2\|_1$. This is equivalent to the classical problem of minimizing the sum of a convex differentiable function and a convex function which is not necessarily differentiable [16]. The solution can be obtained using proximal gradient descent [17] and the algorithm is described in Algorithm 1 where $L = \|\mathbf{D}_1^{(2)^T}\mathbf{D}_1^{(2)} + \mathbf{D}_2^{(2)^T}\mathbf{D}_2^{(2)}\|$ is the Lipschitz constant of $\nabla F(\mathbf{q}_1, \mathbf{q}_2)$ and $\mathrm{prox}_f(\cdot)$ is the proximal map of f. The algorithm converges at a rate $O(1/p^2)$ for a fixed step size $p \in (0, 1/L)$ [17, 18].

Once the trajectory is obtained, k-space data is acquired by taking a non-uniform Fourier transform (NFT) along this trajectory for the test images. This k-space data is then used to reconstruct the images back as described in the next section.

3. SIMULATIONS AND RESULTS

3.1. Image reconstruction

The MRI images are sparse in the finite difference domain and wavelet domain [2]. Hence, with incoherent sampling, images can be reconstructed using:

$$\hat{\mathbf{X}} = \underset{\mathbf{X}}{\mathrm{argmin}} \ \|\mathrm{NFT}(\mathbf{X}) - \mathbf{Y}\|_2^2 + \lambda_1\|\mathcal{W}(\mathbf{X})\|_1 + \lambda_2\|\mathbf{X}\|_{\mathrm{TV}}$$

where $\mathbf{Y}$ is the observed k-space data, $\mathcal{W}(\cdot)$ is the wavelet transform and $\|\cdot\|_{\mathrm{TV}}$ is the total variation (TV) norm. This is solved using non-linear conjugate gradient with a fast and cheap backtracking line-search [2, 19]. λ_1 and λ_2 are taken as 0.01 for the reconstruction of the phantom and the MRI images. A Daubechies-4 wavelet is used as the sparsifying basis and the NFT is calculated using the NUFFT package by Fessler [20].

3.2. Simulation setup

To evaluate the COLT method, we consider the reconstruction of two test images of size 256×256, a realistic analytical brain phantom image [21] and a T1-weighted sagittal brain MRI image (obtained using Cartesian imaging). The maximum gradient magnitude $G_{\max}$ and slew rate $S_{\max}$ are taken as 40mT/m and 200mT/m/ms, respectively. The sampling frequency is taken to be 250MHz. Two types of trajectories are created using the COLT method: (a) TSP-based, and (b) random-like trajectories. These are compared with TSP-based trajectories using the TOC and the projection methods. For both trajectories, samples from the k-space are taken from density $\propto 1/|k|^2$ as before. For TSP-based trajectories, the shortest path is found through these sampled points and that is taken as $\mathbf{c}$ in Eq. (3). For random-like trajectories for the COLT method, the sampled points are taken directly as $\mathbf{c}$ in any random order. Comparisons of the methods are done based on the readout time, SSIM and PSNR for the reconstructed images. The performance measures are averaged over 100 trials (different set of random points in each trial) for all methods and are summarized in Table 1. For the TOC method, the number of initial sample points is 2500. For the projection and the COLT method the number of initial sample points is 16384 (25% of 256×256) leading to a total of about 1000 iterations to converge in both methods.

3.3. Simulation results and discussion

Figure 2 shows sample trajectories obtained by different methods and corresponding reconstructed phantom and MRI images. For the projection method, the velocity for CVP is adjusted to have a readout time close to that of the TOC method, which was found to be $0.5v_{\max}$. For the COLT method, it was observed that the performance becomes poorer as λ increases with little reduction in readout time. Hence, λ is chosen as 1. The velocity for CVP for COLT with TSP is taken as $0.25v_{\max}$ such that the performance is close to the projection method. For COLT with random-like trajectories, the velocity for CVP is chosen as $v_{\max}$ as it was observed that the performance did not improve much for a lower velocity. The simulations using the algorithm confirm that the gradient constraints are satisfied in the COLT method. It is observed that the COLT with random-like trajectories outperforms the TOC and projection methods. In terms of readout time, the trajectories obtained by the COLT method are more than 40% faster than the TOC method and the projection method. The COLT method with random-like trajectories performs better

Method	# shots	Readout time (ms)		Phantom image				MRI image			
				SSIM		PSNR (dB)		SSIM		PSNR (dB)	
		Mean	S.D.	Mean	S.D.	Mean	S.D.	Mean	S.D.	Mean	S.D.
TOC	1	133.35	1.41	0.8131	0.0008	28.59	0.30	0.8325	0.0011	29.94	0.38
	2	89.95	0.91	0.8628	0.0108	29.89	0.23	0.8566	0.0045	30.72	0.13
	4	54.00	0.61	0.8918	0.0114	30.89	0.29	0.8699	0.0043	31.17	0.14
Projection	1	137.13	0.60	0.5352	0.0840	23.53	3.55	0.6105	0.0747	25.82	2.75
	2	86.51	0.40	0.6492	0.1135	26.30	3.41	0.6892	0.0759	27.15	1.60
	4	52.31	0.18	0.4692	0.0784	19.55	2.26	0.5382	0.0794	23.27	2.21
COLT TSP	1	**75.21**	1.06	0.5742	0.0786	24.53	3.09	0.6557	0.0790	26.85	3.22
	2	**48.73**	0.56	0.7295	0.0686	27.32	1.36	0.7433	0.0462	27.48	0.90
	4	**29.26**	0.31	0.6100	0.1260	23.84	3.68	0.6604	0.0940	26.56	2.43
COLT random	1	**61.59**	0.36	**0.8893**	0.0760	**30.11**	2.09	**0.8728**	0.0877	**29.55**	2.79

Table 1: Mean and standard deviation (S.D.) of readout time, SSIM and PSNR over 100 trials for the brain phantom and MRI image reconstructions using different methods under single and multi-shot schemes to obtain feasible trajectories.

than all other methods as it contains overlapping in the trajectories and this results in much denser sampling of the center of the k-space.

For random-like trajectories, it was observed that out of 100 trials, 42 trajectories resulted in an SSIM higher than 0.95 and about 17 trajectories resulted in an SSIM less than 0.8 for brain phantom image. This happens because there is a lot of randomness involved and for practical purposes, a trajectory that leads to a higher SSIM during simulations is proposed to be used.

The proposed method provides a way to obtain a feasible trajectory from an otherwise infeasible trajectory, such as a TSP-based one. For a more generally used spiral trajectory, we would like to mention that the projection-based methods (COLT and the projection method) perform better in reconstruction as compared to the TOC method at the cost of increasing the readout time. This is because the initial set of points is critical in the spiral trajectory for projection-based methods. The trajectory could be distorted wherever the physical constraints are not satisfied. Hence, to avoid this, the fraction of $v_{\max}$ for CVP needs to be small for the projection method and the initial points need to be interpolated at a high rate for the COLT method. This results in more sample points and hence in a better reconstruction [22].

3.4. Multi-shot trajectories

A readout time of about 140 ms (in case of TSP trajectories) is not practical for MRI due to subsequent loss in signal strength, off-resonance effects and other acquisition errors. Hence, it is more useful to acquire different regions of k-space in multiple RF excitations. This is known as multi-shot acquisition. Multi-shot (2-shot and 4-shot) TSP-based curves with some overlap between the trajectories are shown in Fig. 3. Simulations were also performed to test the performance of various methods in the multi-shot scenario as shown in Table 1. Note that the readout time displayed is per-shot and the total scan time will depend on the repetition time (TR) and will be $2 \times$ TR and $4 \times$ TR in the 2-shot and 4-shot cases, respectively. For the 2-shot trajectories, the
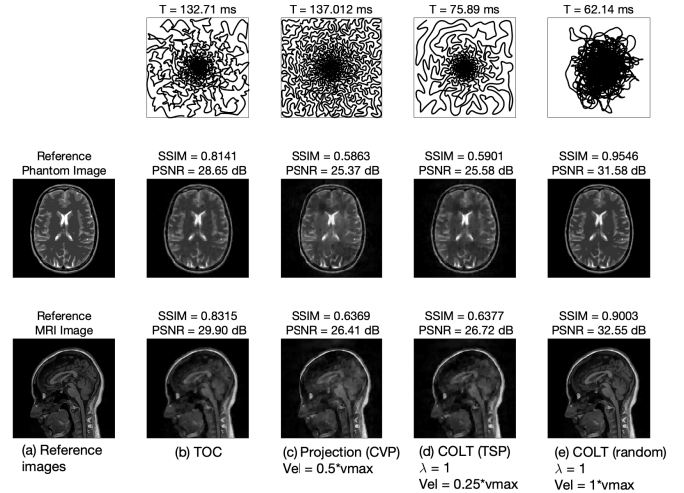

Fig. 2: (a) Reference images used for simulations (brain phantom image and MRI image). Trajectories and reconstructed reference images using (b) TOC method, (c) projection method, (d) COLT with TSP method, (e) COLT with random method.
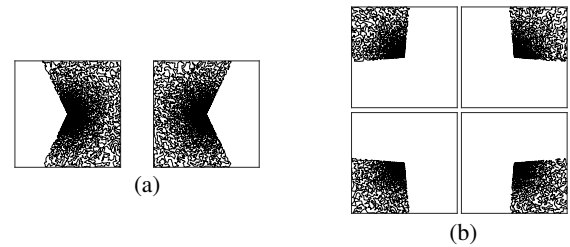

Fig. 3: Multi-shot TSP trajectories: (a) 2-shot, and (b) 4-shot.

readout time is more than 85 ms for the TOC and projection methods, whereas the readout time for the COLT with TSP method is about 48 ms with an improvement in reconstruction performance compared to the projection method. For the 4-shot trajectories, the readout time for the TOC and projection methods is about 50 ms whereas it is about 30 ms for the COLT with TSP method. Here also, the performance improves compared to the projection method.

4. CONCLUSION

We have provided an alternative method for obtaining much faster and feasible k-space sampling trajectories in MRI. We have shown the effectiveness of interpolating the trajectory post-projection in reducing the readout time for TSP-based and random-like trajectories. The method consists of solving a constrained convex optimization problem for which an iterative algorithm in the dual space has been provided. The resultant curve is then constant velocity parameterized to obtain a continuous trajectory which is much shorter than the TOC and the projection methods. The proposed method provides an acceleration of about 50% which is significant. The proposed method also gives the designer the freedom to choose the weighting parameter in order to tune the trade-off between readout time and reconstruction performance.

5. REFERENCES

[1] Richard B Buxton, *Introduction to functional magnetic resonance imaging: principles and techniques*, Cambridge University Press, 2009.

[2] Michael Lustig, David Donoho, and John M Pauly, "Sparse MRI: The application of compressed sensing for rapid MR imaging," *Magnetic Resonance in Medicine*, vol. 58, no. 6, pp. 1182–1195, 2007.

[3] Mark A Griswold, Peter M Jakob, Robin M Heidemann, Mathias Nittka, Vladimir Jellus, Jianmin Wang, Berthold Kiefer, and Axel Haase, "Generalized autocalibrating partially parallel acquisitions (GRAPPA)," *Magnetic Resonance in Medicine*, vol. 47, no. 6, pp. 1202–1210, 2002.

[4] Klaas P Pruessmann, Markus Weiger, Markus B Scheidegger, Peter Boesiger, et al., "SENSE: sensitivity encoding for fast MRI," *Magnetic Resonance in Medicine*, vol. 42, no. 5, pp. 952–962, 1999.

[5] Katherine L Wright, Jesse I Hamilton, Mark A Griswold, Vikas Gulani, and Nicole Seiberlich, "Noncartesian parallel imaging reconstruction," *Journal of Magnetic Resonance Imaging*, vol. 40, no. 5, pp. 1022–1040, 2014.

[6] David S Smith, Lori R Arlinghaus, Thomas E Yankeelov, and Edward B Welch, "Curvelets as a sparse basis for compressed sensing magnetic resonance imaging," in *Medical Imaging 2013: Image Processing*. International Society for Optics and Photonics, 2013, vol. 8669, p. 866929.

[7] Saiprasad Ravishankar and Yoram Bresler, "MR image reconstruction from highly undersampled k-space data by dictionary learning," *IEEE Transactions on Medical Imaging*, vol. 30, no. 5, pp. 1028, 2011.

[8] Michael Lustig, Jin Hyung Lee, David L Donoho, and John M Pauly, "Faster imaging with randomly perturbed, under-sampled spirals and l1 reconstruction," in *Proceedings of the 13th annual meeting of ISMRM*, 2005, p. 685.

[9] Ti-Chiun Chang, Lin He, and Tong Fang, "MR image reconstruction from sparse radial samples using bregman iteration," in *Proceedings of the 13th Annual Meeting of ISMRM*, 2006, vol. 696, p. 482.

[10] Ben Adcock, Anders C Hansen, Clarice Poon, and Bogdan Roman, "Breaking the coherence barrier: asymptotic incoherence and asymptotic sparsity in compressed sensing," *preprint*, 2013.

[11] Nicolas Chauffert, Philippe Ciuciu, Jonas Kahn, and Pierre Weiss, "Variable density sampling with continuous trajectories. Application to MRI," *SIAM Journal on Imaging Sciences*, vol. 7, no. 4, pp. 1962–1992, 2014.

[12] Nicolas Chauffert, Philippe Ciuciu, Jonas Kahn, and Pierre Weiss, "Travelling salesman-based variable density sampling," *Proceedings of the 10th SampTA Conference*, pp. 509–512, 2013.

[13] Michael Lustig, Seung-Jean Kim, and John M Pauly, "A fast method for designing time-optimal gradient waveforms for arbitrary k-space trajectories," *IEEE Transactions on Medical Imaging*, vol. 27, no. 6, pp. 866–873, 2008.

[14] Mathias Davids, Michaela Ruttorf, Frank G Zöllner, and Lothar R Schad, "Fast and robust design of time-optimal k-space trajectories in MRI," *IEEE Transactions on Medical Imaging*, vol. 34, no. 2, pp. 564–577, 2015.

[15] Nicolas Chauffert, Pierre Weiss, Jonas Kahn, and Philippe Ciuciu, "A projection algorithm for gradient waveforms design in magnetic resonance imaging," *IEEE Transactions on Medical Imaging*, vol. 35, no. 9, pp. 2026–2039, 2016.

[16] Yu Nesterov, "Smooth minimization of non-smooth functions," *Mathematical programming*, vol. 103, no. 1, pp. 127–152, 2005.

[17] Neal Parikh, Stephen Boyd, et al., "Proximal algorithms," *Foundations and Trends® in Optimization*, vol. 1, no. 3, pp. 127–239, 2014.

[18] Yurii Nesterov, "A method of solving a convex programming problem with convergence rate O(1/k2)," in *Soviet Mathematics Doklady*, 1983, vol. 27, pp. 372–376.

[19] M Lustig, "SparseMRI toolbox downloaded from http://www.eecs.berkeley.edu/m̃lustig/software.html," 2014.

[20] Jeffrey A Fessler and Bradley P Sutton, "Nonuniform fast fourier transforms using min-max interpolation," 2003.

[21] Matthieu Guerquin-Kern, L Lejeune, Klaas Paul Pruessmann, and Michael Unser, "Realistic analytical phantoms for parallel magnetic resonance imaging," *IEEE Transactions on Medical Imaging*, vol. 31, no. 3, pp. 626–636, 2012.

[22] Nicolas Chauffert, *Compressed Sampling along physically plausible trajectories MRI*, Ph.D. thesis, Paris 11, 9 2015.